MAE494

Project 2

Sam Jackson

11/17/2021 (12/8/2021 creation of word version, originally created in as an ipynb)

Problem Statement

The design of the currently existing brake disc, isometrically shown in Figure 1 and shown in profile view in Figure 2, should be optimized for emergency braking conditions with minimal volume using ANSYS' simulation and optimization tools. To simplify this optimization only three geometrical parameters, the rotor disc thickness of 25mm (H28), outer diameter of 75mm (V29), and inner diameter of 125mm (V30) of the disc, are to be changed. To survive the emergency braking conditions the design should aim to minimize the maximum stress in the brake disc, maximize the first natural frequency of the brake disc, and minimize the maximum temperature in the disc.

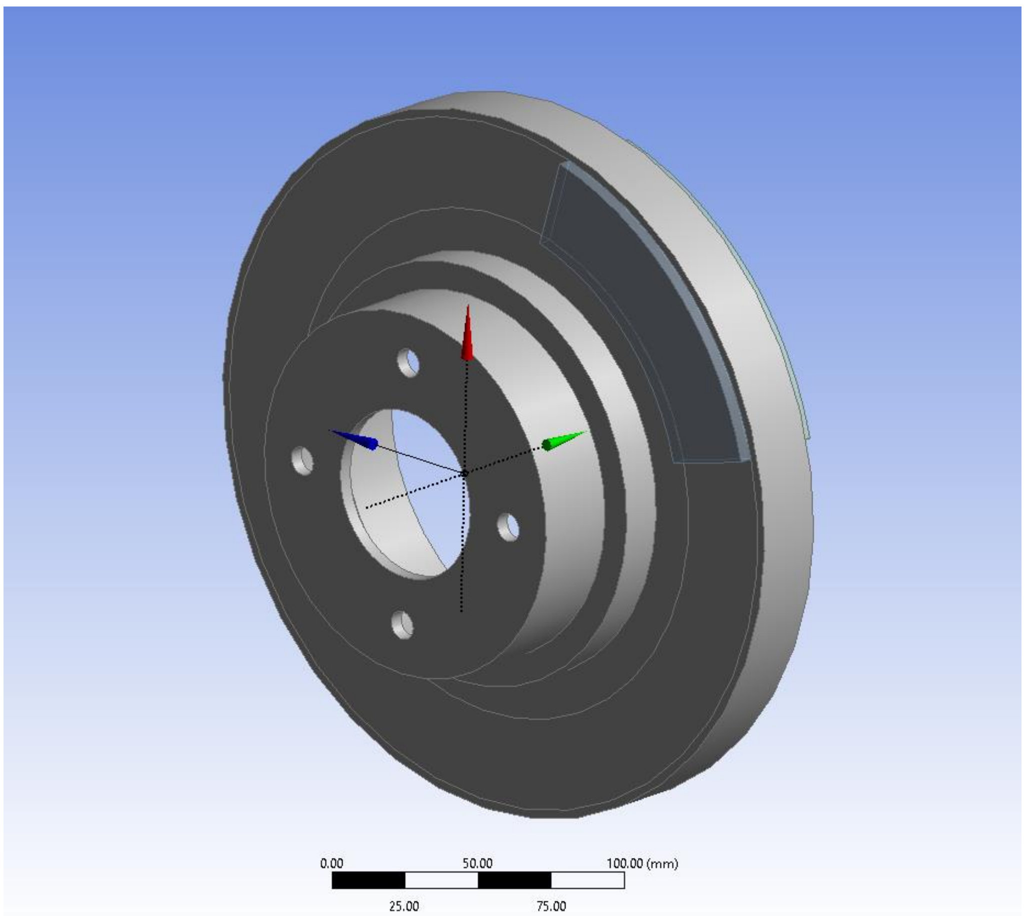

Figure 1: Isometric View of Initial Brake Disc

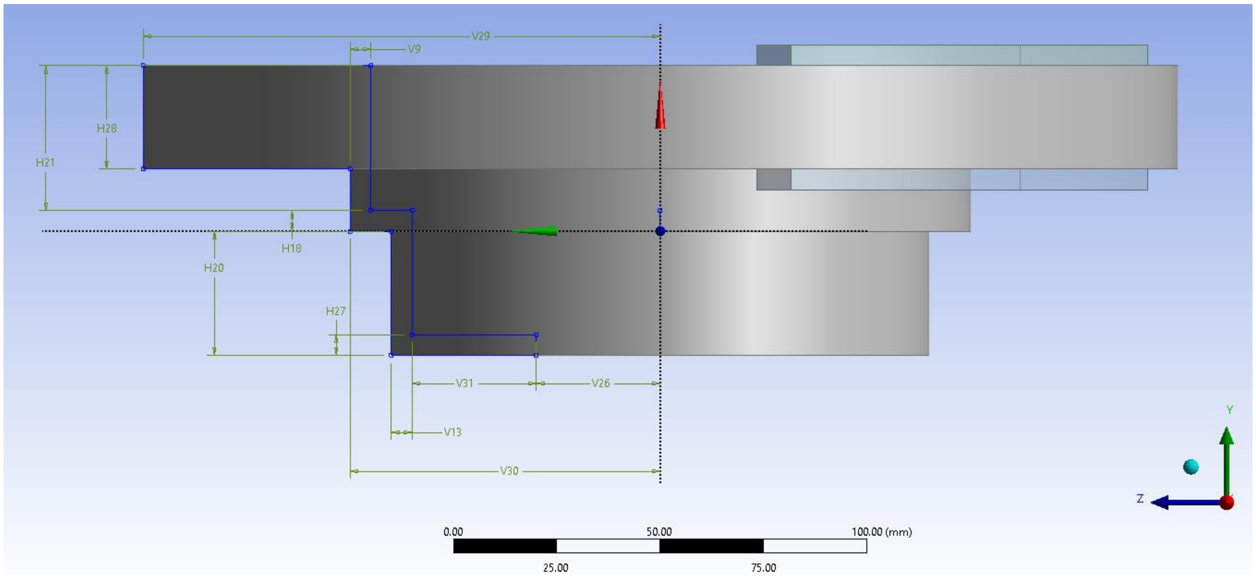

Figure 2: Profile View of Initial Brake Disc

Setup of Analysis

To conduct this optimization of the brake disc, three types of analysis were to be conducted on the brake disc designs during simulated operation, detailed in the Project 2 document. The three analyses performed on the designs were Structural Analysis, Modal Analysis and Thermal Analysis to find the maximum von-Mises stress, first natural frequency, and maximum temperature in the disc, respectively. These three variables were set to be output parameters in ANSYS, to later be used for optimization. Similarly, the three geometric parameters of the disc were also set to be parameters controllable by optimization tools, however these were set to be input parameters rather than output parameters. The result of creating these parameters is shown in Figure 3.

	A	B	C	D
	Outline of All Parameters			
1	ID	Parameter Name	Value	Unit
2	⊟ Input Parameters			
3	⊟ Static Structural (A1)			
4	P1	rotor_thickness	25	mm
5	P2	rotor_OD	125	mm
6	P3	rotor_ID	75	mm
*	New input parameter	New name	New expression	
8	⊟ Output Parameters			
9	⊟ Static Structural (A1)			
10	P4	Equivalent Stress Maximum	1.2647E+07	Pa
11	P7	Solid Volume	0.00099667	m^3
12	⊟ Modal (B1)			
13	P5	Total Deformation Reported Frequency	1590.4	Hz
14	⊟ Transient Thermal (C1)			
15	P6	Temperature Maximum	335.38	C
*	New output parameter		New expression	
17	Charts			

Figure 3: Outline of Input and Output Parameters of the Brake Disc

Design of Experiments

To find the optimal design, the design space of the brake disc was explored by sampling the output parameters, or the results of the analyses, across the wide continuous range of input parameters, or different designs of the brake disc. Since there are limitations on the feasible dimensions of the brake disc, as well as a limit on the number of nodes that can be used in simulation (due to the use of the student version of ANSYS), the full design space cannot be explored, however a reasonable portion of it can be. Thus, the upper and lower bounds of the geometric parameters that limit this smaller feasible design space were decided and implemented into the simulation. These chosen bounds and the reasons for their choice are shown in Table 1, shown below.

Table 1: Upper and Lower Bounds of Input Parameters and Their Active Constraints

	Rotor Thickness		**Rotor Outer Diameter**		**Rotor Inner Diameter**	
Lower Bound	15 mm	No Major Constraint	123 mm	Geometric Constraint	66 mm	Geometric Constraint
Upper Bound	26.5 mm	Node Limit	160 mm	Node Limit	85 mm	Node Limit

To efficiently explore this defined space without needing an immense amount of sample points, and thus an immense amount of simulations, a Latin Hypercube Sampling process was used. Originally only 10 and then 20 points were used to sample the space, however this was found to be not enough to get an accurate fit to the data (shown in the Response Surface section), so instead 50 points were used to sample the bound space. These 50 points and their respective output parameters calculated through simulation are shown in Figures 4 and 5, shown below.

1	Name	P1 - rotor_thickness (mm)	P2 - rotor_OD (mm)	P3 - rotor_ID (mm)	P4 - Equivalent Stress Maximum (Pa)	P5 - Total Deformation Reported Frequency (Hz)	P6 - Temperature Maximum (C)	P7 - Solid Volume (m^3)
2	1	19.07	125.59	84.43	1.1636E+07	1295.8	361.81	0.00076315
3	2	21.05	147.05	73.79	1.2318E+07	1112.6	347.06	0.001277
4	3	15.33	154.45	67.71	1.1648E+07	820.91	396.48	0.001115
5	4	19.95	144.83	84.05	1.7458E+07	1063.9	353.35	0.0011157
6	5	15.77	131.51	69.23	1.0615E+07	1263.8	390.76	0.00081125
7	6	25.23	134.47	77.59	1.2923E+07	1380.9	332.5	0.0011764
8	7	19.73	150.01	83.29	1.8553E+07	995.89	354.67	0.0012058
9	8	25.01	145.57	66.19	1.2956E+07	1223.6	333.11	0.0015028
10	9	17.09	136.69	71.89	1.0906E+07	1205.5	375.78	0.00092635
11	10	16.43	159.63	68.09	1.3083E+07	793.17	382.64	0.0012641
12	11	17.97	123.37	68.85	1.0723E+07	1538.8	375.78	0.00078225
13	12	16.21	141.13	74.55	1.1445E+07	1099.5	385.29	0.00094101
14	13	18.85	139.65	71.13	1.106E+07	1190.9	360.59	0.0010534
15	14	21.71	157.41	73.03	1.5449E+07	975.25	343.85	0.0015307
16	15	17.75	130.03	84.81	1.197E+07	1228.1	369.82	0.00078843
17	16	23.69	152.23	81.77	1.8371E+07	1038.9	336.59	0.0014625
18	17	23.25	141.87	69.61	1.1926E+07	1258	337.71	0.0013093
19	18	20.83	158.15	81.01	1.8873E+07	921.47	348.15	0.0014399
20	19	15.99	138.17	76.83	1.0877E+07	1152.7	388.03	0.00088014
21	20	15.55	158.89	78.35	1.5349E+07	817.57	393.36	0.0011565
22	21	18.63	146.31	75.31	1.2145E+07	1068.7	362.22	0.0011333
23	22	23.91	129.29	81.39	1.26E+07	1375.7	335.85	0.00099203
24	23	25.45	155.19	79.49	2.1058E+07	1051.9	331.63	0.0016475
25	24	16.65	127.81	73.41	1.0788E+07	1396.3	381.43	0.00077839
26	25	22.37	142.61	68.47	1.1843E+07	1218.6	341.33	0.0012892

Figure 4: First 25/50 Design Points Used in DOE

1	Name	P1 - rotor_thickness (mm)	P2 - rotor_OD (mm)	P3 - rotor_ID (mm)	P4 - Equivalent Stress Maximum (Pa)	P5 - Total Deformation Reported Frequency (Hz)	P6 - Temperature Maximum (C)	P7 - Solid Volume (m^3)
27	26	20.61	137.43	76.45	1.1686E+07	1260.1	349.32	0.0010608
28	27	23.03	135.95	79.87	1.542E+07	1290.4	338.97	0.0011042
29	28	21.49	128.55	71.51	1.1363E+07	1493.4	345.32	0.00096982
30	29	25.67	135.21	67.33	1.1403E+07	1447.8	331.18	0.0012944
31	30	18.19	151.49	76.07	1.359E+07	977.39	365.69	0.0011958
32	31	22.59	153.71	70.75	1.5421E+07	1047.4	340.11	0.0015184
33	32	23.47	150.75	66.95	1.347E+07	1102.5	337.17	0.0015296
34	33	19.29	138.91	77.97	1.1393E+07	1199.4	357.28	0.0010226
35	34	24.13	149.27	80.63	1.7227E+07	1094.3	334.99	0.0014275
36	35	18.41	152.97	77.21	1.4802E+07	960.01	363.96	0.0012276
37	36	17.31	126.33	69.99	1.1106E+07	1447.6	375.73	0.00079584
38	37	24.79	143.35	75.69	1.4319E+07	1240.5	333.37	0.0013679
39	38	24.57	132.25	80.25	1.3239E+07	1362.2	334.11	0.0010828
40	39	20.39	124.11	74.93	1.0679E+07	1534.2	355.56	0.00083807
41	40	25.89	156.67	78.73	2.0433E+07	1045.8	330.54	0.0017167
42	41	20.17	132.99	72.65	1.0715E+07	1360.8	352.22	0.0009895
43	42	19.51	155.93	72.27	1.6601E+07	943.01	355.98	0.0013721
44	43	21.93	127.07	70.37	1.1334E+07	1543.3	344.14	0.00096688
45	44	16.87	133.73	82.15	1.0895E+07	1205.8	378.12	0.00082693
46	45	22.81	130.77	83.67	1.3999E+07	1298.8	339.75	0.00096619
47	46	22.15	147.79	82.91	1.8479E+07	1064.6	341.82	0.0012811
48	47	24.35	124.85	74.17	1.1528E+07	1597.3	337.54	0.00098
49	48	21.27	140.39	66.57	1.1592E+07	1216.9	345.85	0.0012041
50	49	17.53	148.53	82.53	1.6636E+07	985.59	371.42	0.001078
51	50	15.11	144.09	79.11	1.24E+07	1025.4	399.5	0.00091422

Figure 5: Second 25/50 Design Points Used in DOE

Response Surface

Using the 50 design points found in the DOE, a response surface was created to illustrate how the output parameters change in response to changes in the input parameters. Multiple methods of creating the response surface, such as Non-parametric Regression and Sparse Grid, were tried, however it was ANSYS's Genetic Aggregation method which yielded the best fit to the data. Thus, it was this Genetic Aggregation method that was used to create the response surface due to its accuracy, ability to provide a good fit with a relatively small number of points, and ability to model non-smooth data.

To test if the fit provided by this method was good, a number of verification points (5 and then 12 points) were created which did not influence the creation of response surface. After this, the goodness of fit of the response surface prediction was tested against both the learning points and the verification points. The 12 verification points used to verify the final DOE learning points are shown in Figure 6, below.

1	Name	P1 - rotor_thickness (mm)	P2 - rotor_OD (mm)	P3 - rotor_ID (mm)	P4 - Equivalent Stress Maximum (Pa)	P5 - Total Deformation Reported Frequency (Hz)	P6 - Temperature Maximum (C)	P7 - Solid Volume (m^3)
2	1	25.815	140.62	84.777	1.753E+07	1199.4	330.75	0.0012673
3	2	25.933	159.42	69.15	1.836E+07	1045.1	330.52	0.0018727
4	3	24.926	123.19	66.172	1.2746E+07	1712.8	339.26	0.0010274
5	4	18.762	149.58	66.573	1.1758E+07	985.93	361.15	0.0012409
6	5	15.669	142.49	66.289	1.0801E+07	997.8	391.86	0.00096545
7	6	20.727	159.92	66.283	1.4964E+07	897.43	348.57	0.0015616
8	7	15.06	157.1	84.521	1.8357E+07	826	400.23	0.0010754
9	8	15.004	123.25	81.956	1.0742E+07	1339.1	411.83	0.00063551
10	9	25.918	159.8	84.911	2.4667E+07	966.23	330.62	0.0017393
11	10	15.106	151.83	73.313	1.1501E+07	886.69	399.53	0.0010445
12	11	17.728	123.97	78.788	1.0698E+07	1431.5	376.17	0.00073473
13	12	18.697	133.14	66.412	1.14E+07	1287.2	361.84	0.0009649

Figure 6: 12 Verification Points Used in Response Surface Verification

Originally the simulations with 10 and 20 DOE learning points were found to have a relatively bad fit to the 10 checked points of verification data, as shown in the goodness of fit plot for 20 points in Figure 6. So, the simulation was run again with the 50 DOE learning points (shown prior) to sample the space which produced a much better fit to the 12 verification points used. The new goodness of fit plot and metrics on the goodness of fit of the response surface are shown in Figures 7 and 8 respectively.

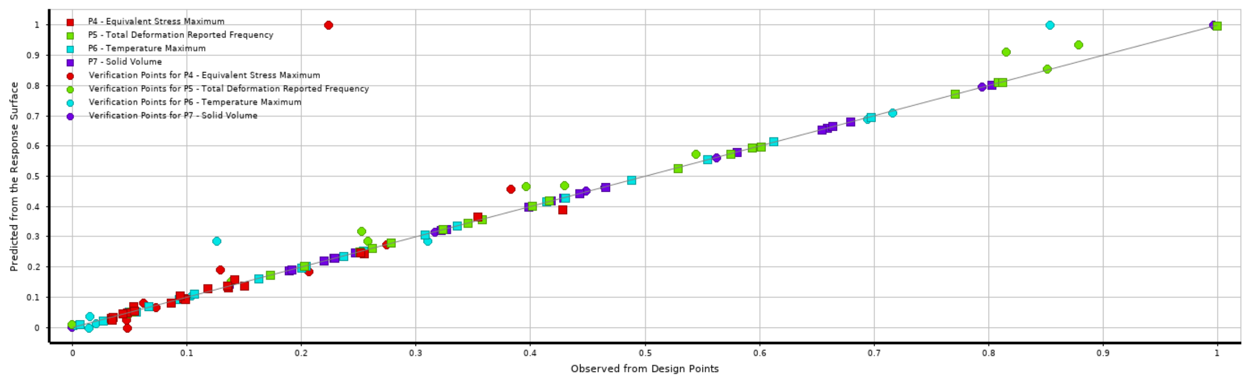

Figure 7: Initial Goodness of Fit Plot with 20 Learning Points

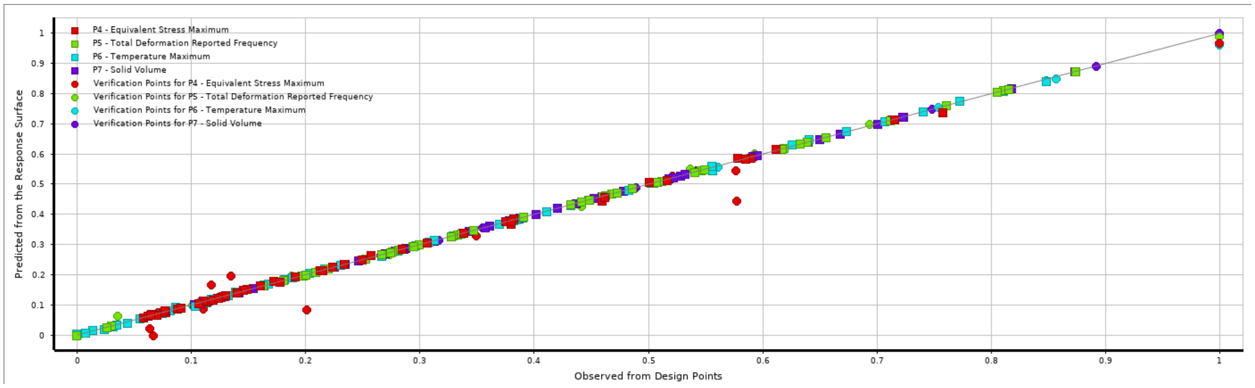

Figure 8: Final Goodness of Fit Plot with 50 Learning Points

	A	B	C	D	E
1		P4 - Equivalent Stress Maximum	P5 - Total Deformation Reported Frequency	P6 - Temperature Maximum	P7 - Solid Volume
2	Coefficient of Determination (Best Value = 1)				
3	Learning Points	0.99933	1	0.9998	1
4	Cross-Validation on Learning Points	0.94328	0.99982	0.99963	1
5	Root Mean Square Error (Best Value = 0)				
6	Learning Points	73282	0.0039203	0.28225	3.8016E-09
7	Verification Points	9.3197E+05	10.49	0.95582	1.6819E-07
8	Cross-Validation on Learning Points	6.7299E+05	2.6346	0.38526	2.9254E-08
9	Relative Maximum Absolute Error (Best Value = 0%)				
10	Learning Points	10.358	0	3.8155	0
11	Verification Points	61.949	12.667	13.957	0.1182
12	Cross-Validation on Learning Points	91.144	4.4434	8.4539	0.05398
13	Relative Average Absolute Error (Best Value = 0%)				
14	Learning Points	1.7311	0	1.1133	0
15	Verification Points	22.889	3.6719	2.399	0.046548
16	Cross-Validation on Learning Points	16.348	0.96611	1.3563	0.006353

Figure 9: Goodness of Fit Quality Metrics for 50 Learning Points

As we can see, the quality metrics of the final response surface fit report that the fit is quite good for all but the stress maximum output parameter. This is likely due to the mesh of the simulation being coarser than is sufficient to accurately find the maximum stress experienced by the brake disc, however this issue cannot be resolved due to the node limit restriction posed by the ANSYS student version. If this access to a full license version of ANSYS was able to be acquired coarsening the mesh and rerunning the Structural Analysis simulations to get more accurate maximum stress data would be the first course of action. Though this is a problem that should be solved to ensure an accurate process, optimization can still be carried out as it relies upon knowing the general trends of the parameters, which the response surface has, whilst not necessarily needing accurate numbers to accompany these trends. Thus, the optimization process was continued to be carried out with a fair amount of confidence

Sensitivity Analysis

To show the relationships between the input and the output parameters, the individual response curves were found at a given response point in the domain and are shown in Figures 10 through Figure 22. The response point at which each of these response curves were created was at the center of the explored design space, shown in Figure 22 below. This method of showing multiple response curves at a given point unfortunately does not fully reflect the response of the parameters but does give an idea of which parameters have complex relationships and which have simpler relationships, such as showing monotonicity.

Note these response curves are grouped by the output parameters to better show how monotonicity trends for these output parameters, such as all solid volume relationships showing monotonicity.

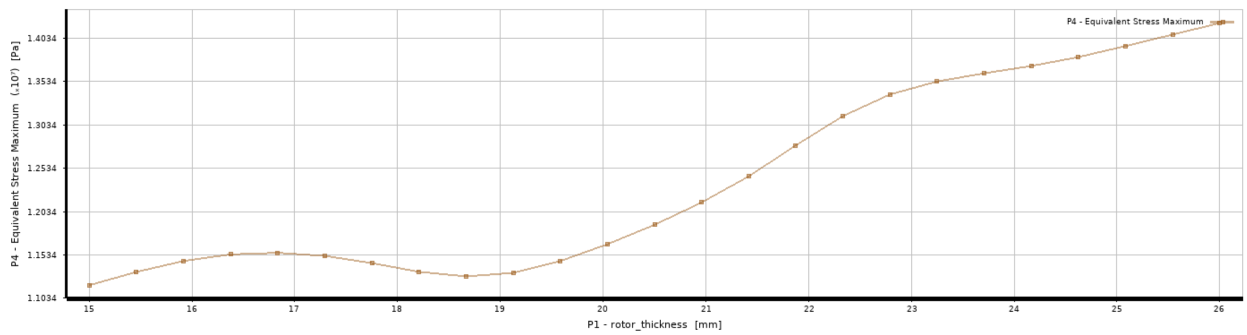

Figure 10: Response Curve for Stress Maximum to Rotor Thickness Changes

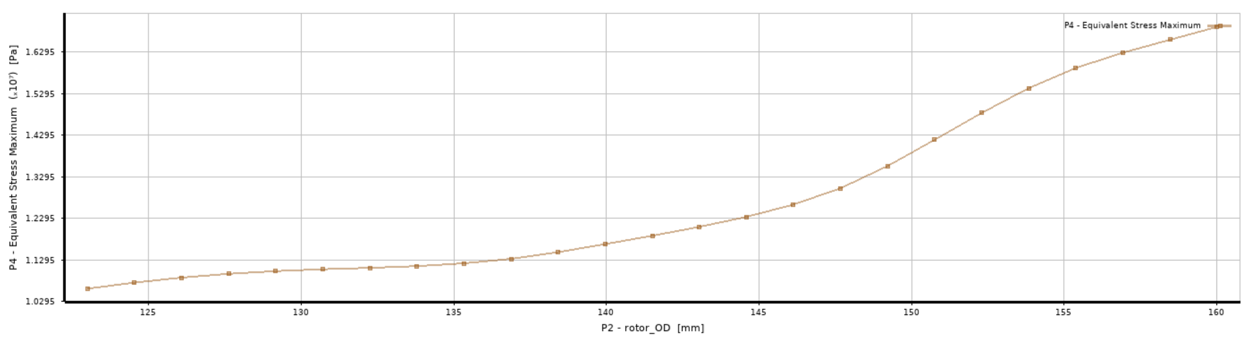

Figure 11: Response Curve for Stress Maximum to Rotor Outer Diameter Changes

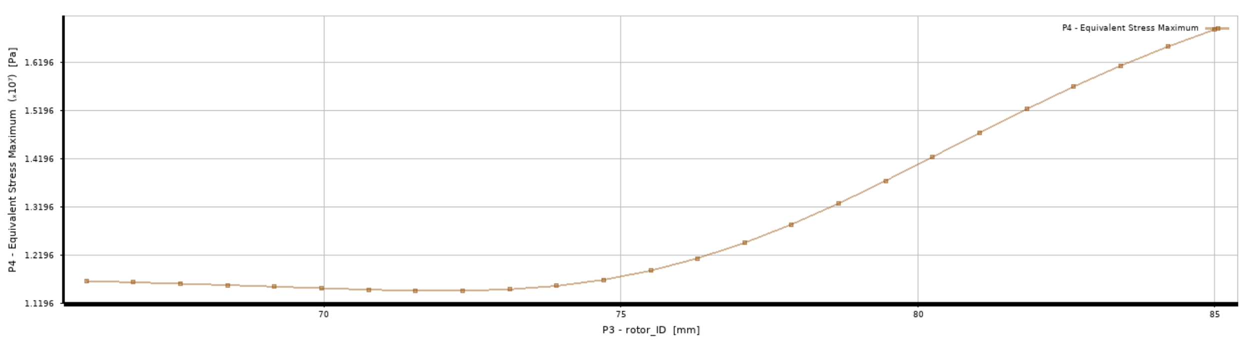

Figure 12: Response Curve for Stress Maximum to Rotor Inner Diameter Changes

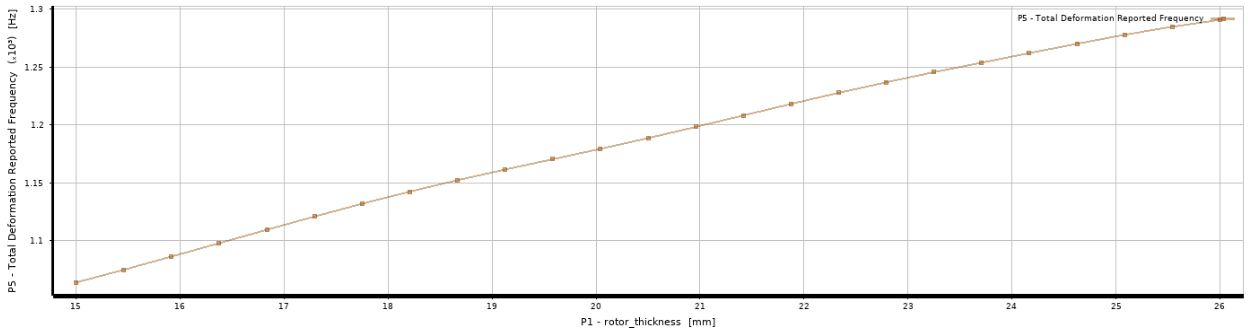

Figure 13: Response Curve for Resonant Frequency to Rotor Thickness Changes

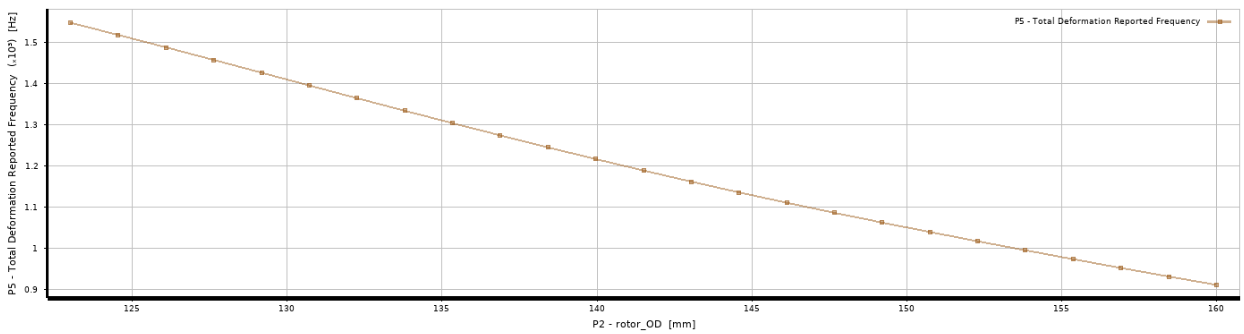

Figure 14: Response Curve for Resonant Frequency to Rotor Outer Diameter Changes

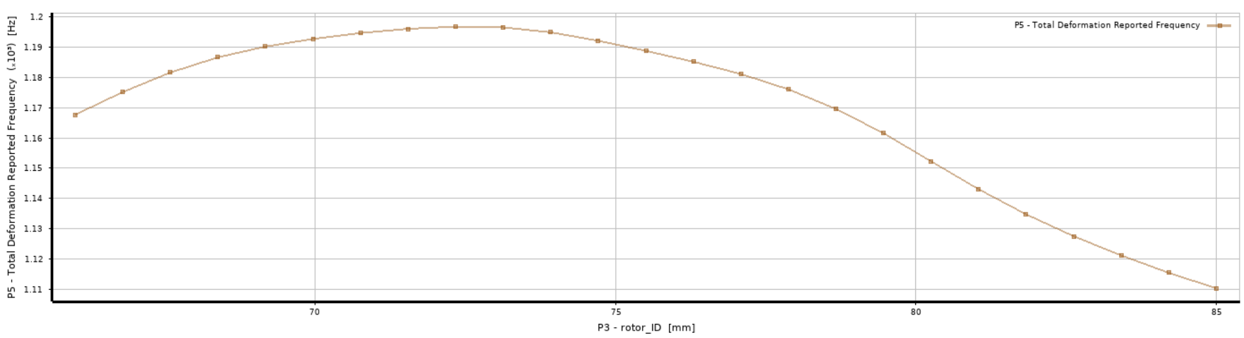

Figure 15: Response Curve for Resonant Frequency to Rotor Inner Diameter Changes

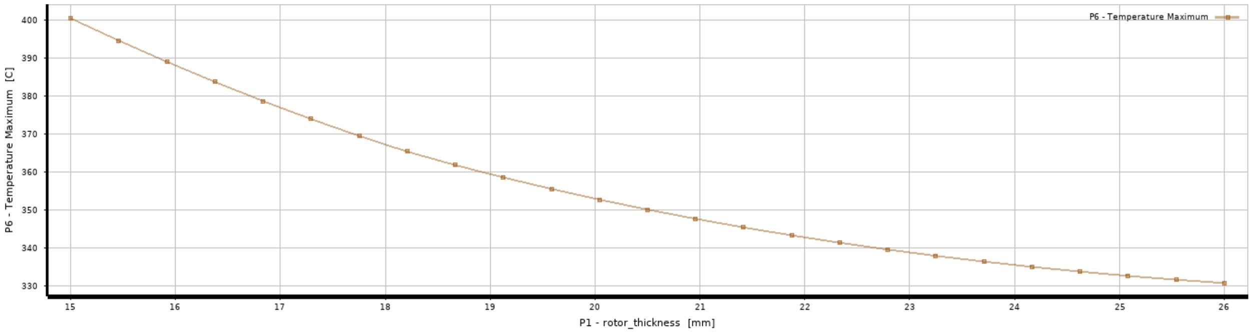

Figure 16: Response Curve for Temperature Maximum to Rotor Thickness Changes

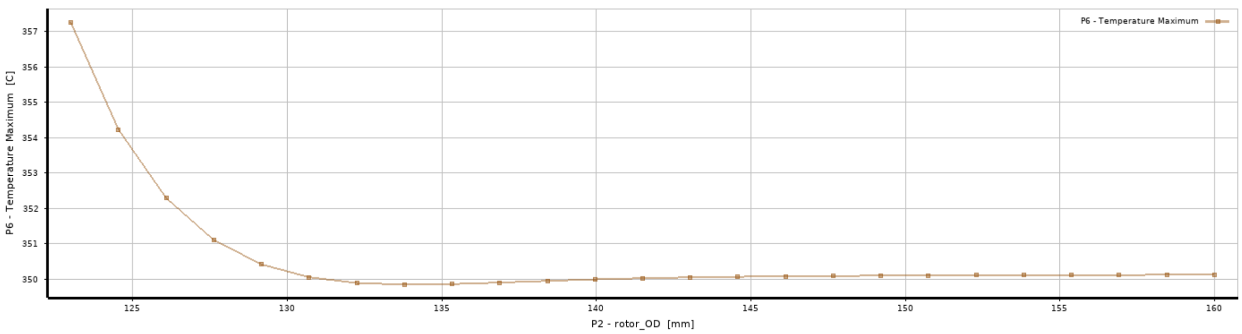

Figure 17: Response Curve for Temperature Maximum to Rotor Outer Diameter Changes

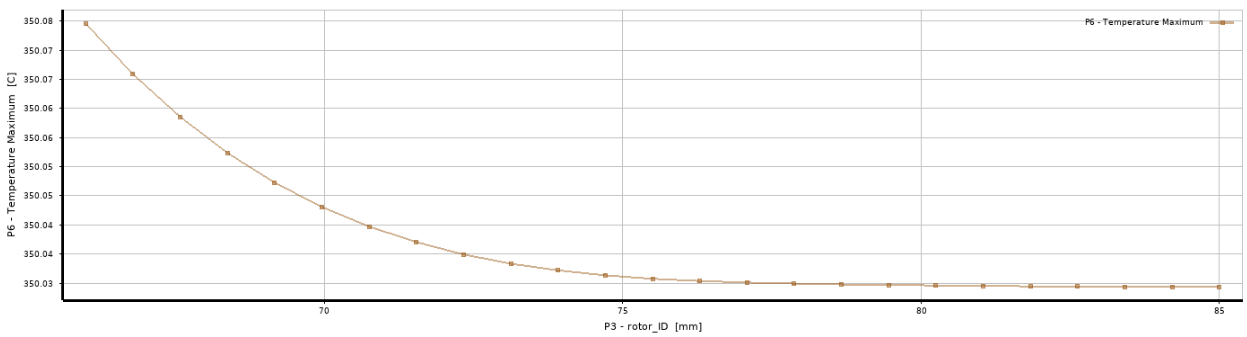

Figure 18: Response Curve for Temperature Maximum to Rotor Inner Diameter Changes

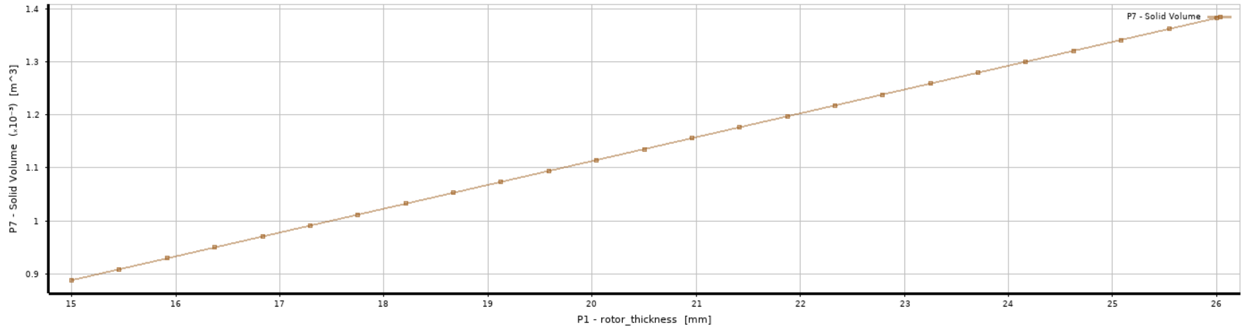

Figure 19: Response Curve for Solid Volume to Rotor Thickness Changes

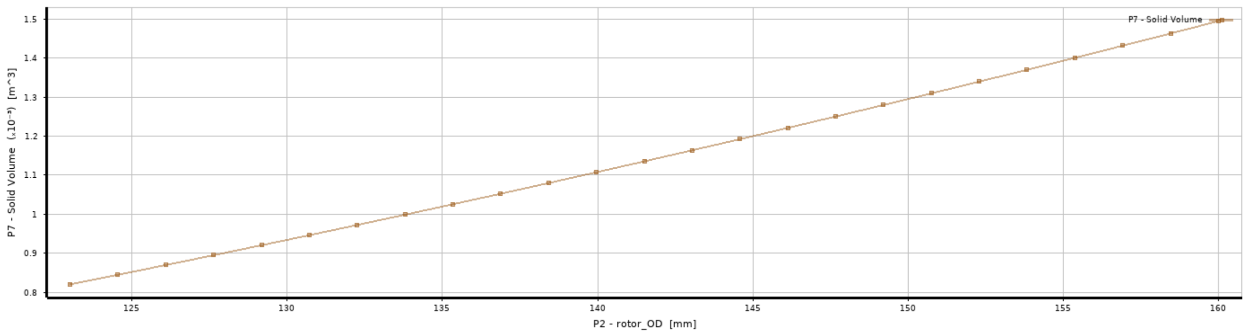

Figure 20: Response Curve for Solid Volume to Rotor Outer Diameter Changes

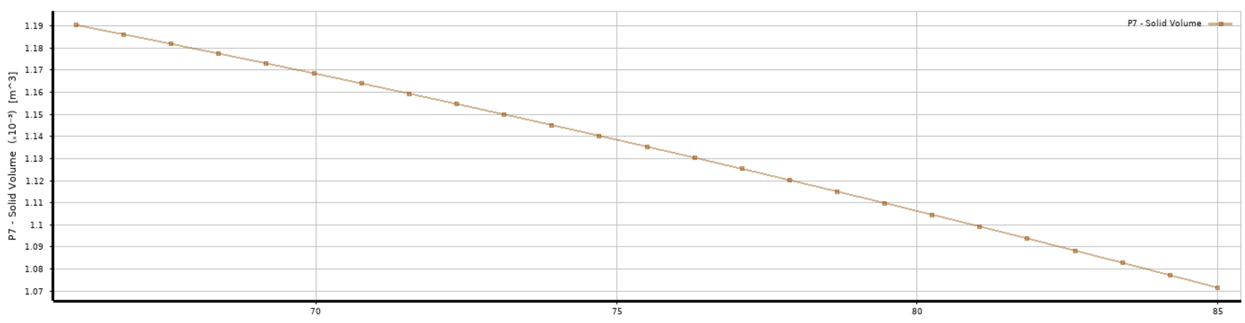

Figure 21: Response Curve for Solid Volume to Rotor Inner Diameter Changes

Name	P1 - rotor_thickness (mm)	P2 - rotor_OD (mm)	P3 - rotor_ID (mm)	P4 - Equivalent Stress Maximum (Pa)	P5 - Total Deformation Reported Frequency (Hz)	P6 - Temperature Maximum (C)	P7 - Solid Volume (m^3)
Response Point	20.5	141.5	75.5	1.1881E+07	1188.7	350.03	0.0011354

Figure 22: Response Point Used in All Previous Response Curves

As we can see from the response curves, all the relationships relating the input parameters to the Stress Maximum and Maximum Temperature are quite complex, while Solid Volume and most (all except Inner Diameter) Resonant Frequency relationships are relatively simple near-linear relationships. These simpler relationships are easy to make physical sense of, as increasing the rotor thickness and rotor outer diameter linearly increases the volume of the brake disc and thus the material available to resist resonating which therefore increases the required resonant frequency. Similar thinking about the mass of the brake disc can also help understand the trends of the maximum temperature and stress relationships. As more rotating mass, created by an increase in the input parameters, requires more force to bring to a halt higher stress is experienced in the disc, whilst having more mass (specifically through the rotor thickness) allows the incoming heat flux from the brake pads to be more widely distributed thus decreasing the maximum temperature experienced by the disc.

By understanding these relationships, we can better understand the tradeoffs of changing the input parameters, such as the fact that decreasing the rotor thickness does give the positives of reducing the solid volume and the stress maximum, however it also gives the negatives of increasing the maximum temperature and reducing the first resonating frequency. These tradeoffs can be very well illustrated by doing a local sensitivity analysis at a given design point to see how the output parameters will change given a small change in the input parameters. Local sensitivity analysis was conducted at the response point used prior and is overall shown in bar graph form in Figure 23 and in individual sensitivity curve form for each of the output parameters in Figures 24 through 27.

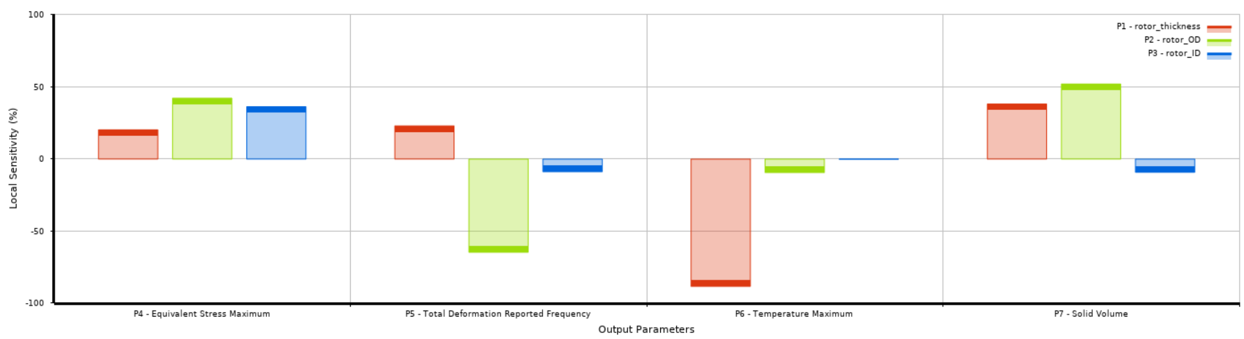

Figure 23: Local Sensitivity Bar Graph at the Response Point

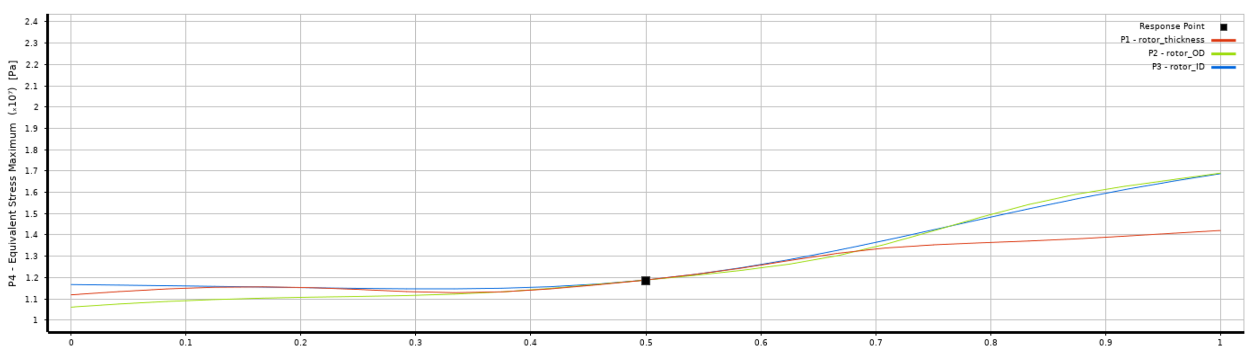

Figure 24: Local Sensitivity Curve for Maximum Stress at the Response Point

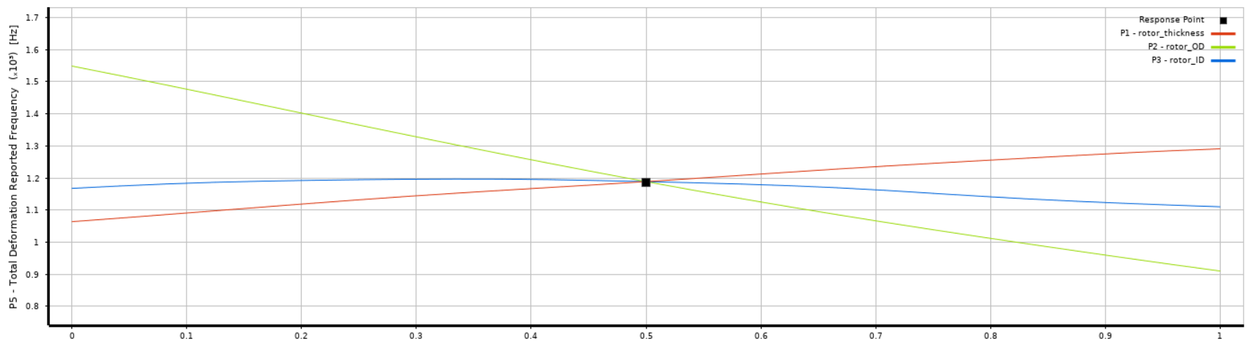

Figure 25: Local Sensitivity Curve for First Resonant Frequency at the Response Point

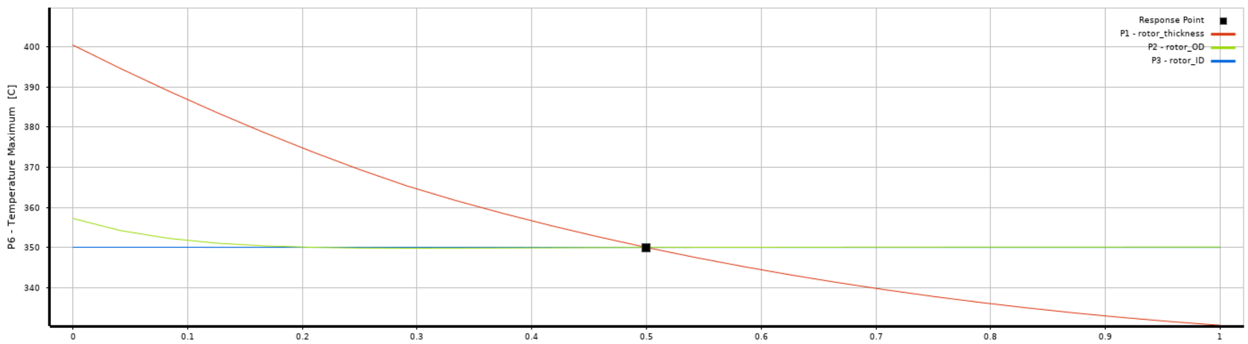

Figure 26: Local Sensitivity Curve for Maximum Temperature at the Response Point

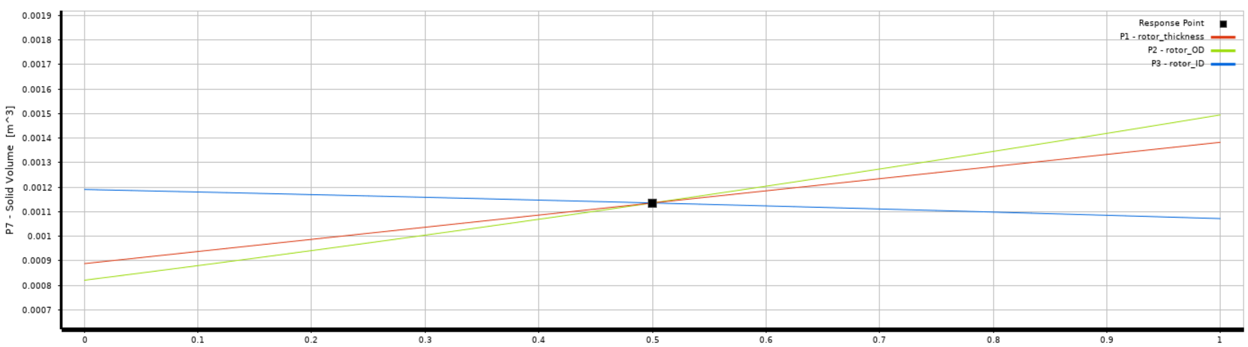

Figure 27: Local Sensitivity Curve for Solid Volume at the Response Point

Optimization

Finally, the created response surface was used to optimize the design via ANSYS's built in Nonlinear Quadratic Programming by Quadratic Lagrangian method. Since the NLPQL method is a single objective method, only one out of the four output parameters can be chosen to be optimized for, whilst the rest of the output parameters are handled via constraints. Since the problem statement seemed to state reducing the volume of the design as the highest priority I chose to use Solid Volume as the objective to minimize, whilst choosing the Stress Maximum, First Resonant Frequency, and Temperature Maximum as inequality constraints with specifically chosen boundaries. I chose the boundaries for these so that two out of the three constraint output parameters would be considered better than the original design, which has output parameters shown in Figure 3. I chose for the Stress Maximum and First Natural Frequency to have the competitive bounds, whilst allowing for the trade-off in Maximum Temperature by setting a boundary higher than the original design, justifying this by the fact that cast-iron has a melting point much higher than anticipated by the simulation. The specific setup of the NLPQL optimization is specified in Figure 28, shown below.

Name	Parameter	Objective			Constraint			
		Type	Target	Tolerance	Type	Lower Bound	Upper Bound	Tolerance
P4 <= 1.25E+07 Pa	P4 - Equivalent Stress Maximum	No Objective			Values <= Upper Bound		1.25E+07	0.001
P5 >= 1600 Hz	P5 - Total Deformation Reported Frequency	No Objective			Values >= Lower Bound	1600		0.001
P6 <= 350 C	P6 - Temperature Maximum	No Objective			Values <= Upper Bound		350	0.001
Minimize P7	P7 - Solid Volume	Minimize	0		No Constraint			

Figure 28: Objectives and Constraints for NLPQL Optimization Setup

With the above setup, the ANSYS optimization setup was run, and three possible candidate designs were found. To ensure that these candidate designs produce accurate results all were then verified (full simulations were run for each design) and the output parameters were recorded and tabulated, as shown in Figure 29 below. Note, while the validated candidate design's output parameters do not precisely fit within the bounds for the optimization, the boundary breaking parameters are close enough not to matter for our purposes.

Name	P1 - rotor_thickness (mm)	P2 - rotor_OD (mm)	P3 - rotor_ID (mm)	P4 - Equivalent Stress Maximum (Pa)		P5 - Total Deformation Reported Frequency (Hz)		P6 - Temperature Maximum (C)		P7 - Solid Volume (m^3)	
				Parameter Value	Variation from Reference	Parameter Value	Variation from Reference	Parameter Value	Variation from Reference	Parameter Value	Variation from Reference
Starting Point	25	141.5	75.5	1.3917E+07	10.05%	1276.7	-19.73%	332.74	-0.79%	0.0013378	34.23%
Candidate Point 1	21.955	123	73.892	1.0948E+07	-13.43%	1600	0.60%	350	4.36%	0.00087438	-12.27%
Candidate Point 1 (verified)				1.2156E+07	-3.88%	1597.7	0.46%	350.96	4.65%	0.00087438	-12.27%
Candidate Point 2	22.003	123.06	72.579	1.0966E+07	-13.29%	1617	1.67%	349.65	4.26%	0.00088566	-11.14%
Candidate Point 2 (verified)				1.2691E+07	0.35%	1618.2	1.75%	350.39	4.48%	0.00088568	-11.14%
Candidate Point 3	22.033	123.09	71.379	1.0979E+07	-13.18%	1629.2	2.44%	349.45	4.20%	0.00089506	-10.19%
Candidate Point 3 (verified)				1.217E+07	-3.76%	1633	2.68%	350.09	4.39%	0.0008951	-10.19%
Original Design	25	125	75	1.1507E+07	-9.01%	1589	-0.09%	336.19	0.24%	0.00099665	0.00%
Original Design (verified)				1.2647E+07	0.00%	1590.4	0.00%	335.38	0.00%	0.00099667	0.00%

Figure 28: Candidate Points, Their Output Parameters, and Their Variation from the Original Design

Since Candidate 1 minimizes the Solid Volume the best whilst mostly fulfilling the constraints, I chose to take it as the final optimized design. As we can see this design with the rotor thickness of 21.955mm, a rotor outer diameter of 123mm, and rotor inner diameter of 73.892mm, not only reduces the Solid Volume by 12.27%, but also reduces the Maximum Stress by 3.88% and increases the First Natural Frequency by 0.6%, with the trade-off of increasing the Maximum Temperature by 4.65%. To confirm that this design is optimal, a local sensitivity analysis was conducted at this design point, shown in Figure 29 below.

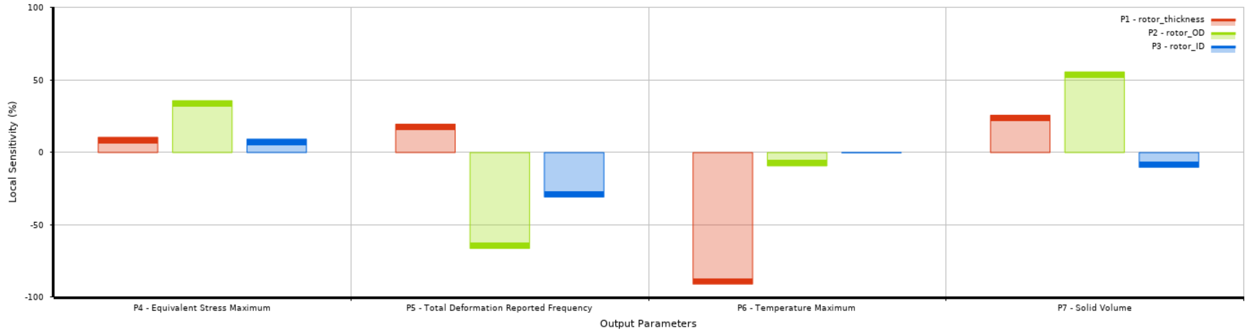

Figure 29: Local Sensitivity Bar Graph of the Final Design

As we can see, this design is quite close to optimal for the explored design space, as any attempt to reduce Solid Volume would result in a violation of constraints. For example, reducing the rotor thickness would massively increase the Temperature Maximum, breaking the constraint, and increasing the rotor inner diameter would not only increase the Maximum Stress but reduce the First Natural Frequency of the disc. The only viable way to change an input parameter to reduce the Solid Volume without massively breaking other constraints would be to reduce the rotor outer diameter, however this is restricted by the geometry of the brake pads, which would lose full contact with the brake disc if it were to become smaller than 122mm. Changing the geometry of these brake pads to allow for a smaller outer diameter of the disc could lead to further improvements of the design.

Thus, the optimization of the design was overall quite successful. It produced a reasonable design which significantly improved two objective parameters, and slightly improved one objective parameter, with the trade off of impairing one objective parameter compared to the original design. This was done through reducing the rotor thickness by ~3mm, reducing the rotor outer diameter by ~2mm, and reducing the inner diameter by ~1.2mm. In addition to the tangible improvements, a direction for further improvements of this design was found through reconsidering the geometry of the brake pads. A comparison of the original design against the optimized design is shown in Figure 30 below.

Initial Design Geometry

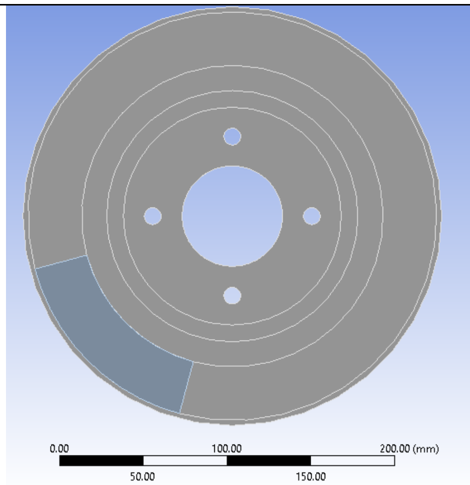

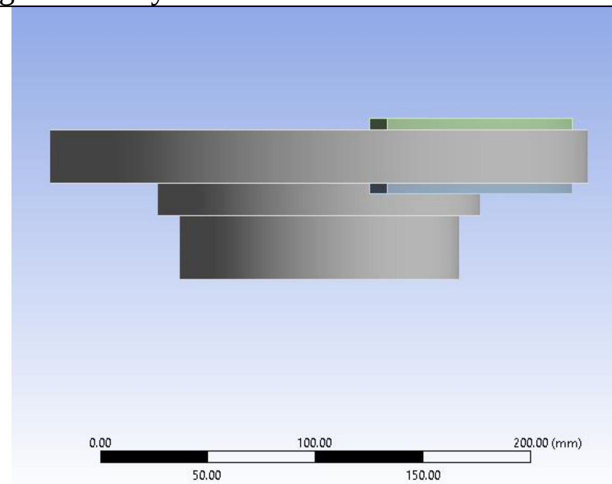

Optimized Design Geometry
with 12.27% Volume Reduction

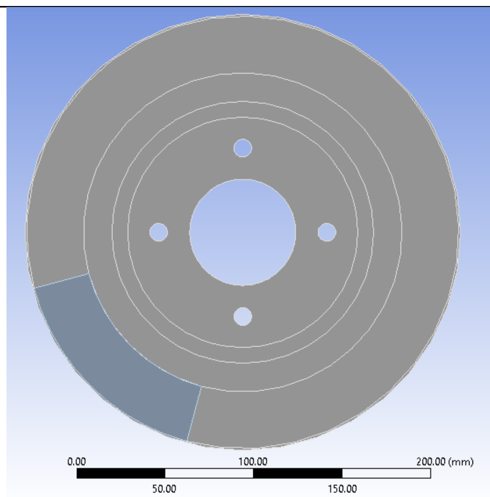

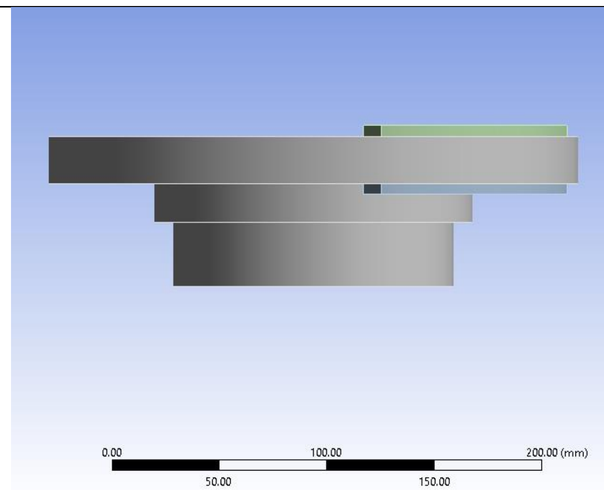

Figure 30: Comparison of Initial and Optimized Design